

Zdzisław PAWLAK\*, Michał GUMINIAK  
Institute of Structural Engineering, Piotrowo 5, 61-138 Poznań

## THE APPLICATION OF FUNDAMENTAL SOLUTIONS IN STATIC ANALYSIS OF THIN PLATES RESTING ON THE INTERNAL ELASTIC SUPPORT

*Received: 5 December 2007*

*Accepted: 20 August 2008*

A static analysis of Kirchhoff plates rested on the elastic internal supports has been discussed in the paper. The Finite Strip Method and Boundary Element Method have been used as an engineering tool in the analysis. Suitable fundamental solutions are applied in these method. Using BEM modified approach, there is no need to introduce the Kirchhoff forces at the plate corner and equivalent shear forces at the plate boundary. Two unknown and independent variables are considered at the boundary element node. The collocation points are located slightly outside the plate boundary, hence the quasi-diagonal integrals of fundamental functions are non-singular. The constant type of boundary element has been used. According to the finite strip method a continuous structure is divided into a set of identical elements simply supported on opposite edges. The unknowns are the deflections and the transverse slope amplitudes along the nodal lines. The difference equation formulation is applied to express the equilibrium conditions of the discrete system. This reduces the number of degrees of freedom to be analyzed. The solution of one equilibrium difference equation yields the fundamental function of the considered plate strip. The fundamental solution derived in this way, can be used to solve the static problem of finite plate in analogically as in the boundary element method for continuous systems.

Key words: Finite Strip Method, Boundary Element Method, Kirchhoff plates, fundamental solutions

---

\* Corresponding author. Tel.: +48-61-665-2471; fax: +48-61-665-2059.

E-mail address: [zdzislaw.pawlak@ikb.poznan.pl](mailto:zdzislaw.pawlak@ikb.poznan.pl) (Z.Pawlak)

## 1. INTRODUCTION

Plates rested on internal elastic supports are often used in building structures. The Finite Strip Method (FSM) and Boundary Element Method (BEM) were created as completely independent numerical tools to solve engineering problems [1], [2]. These methods are the alternative way to the most popular Finite Element Method. The application of FSM and BEM does not require many degrees of freedom and all domain discretization but the boundary of a considered structure only (BEM). BEM reduces the computational dimension by one. The selection of the BEM for the analysis of structures requires searching and applying of some types of functions called fundamental functions or fundamental solutions. The fundamental solution describes a behavior of an infinite structure in the sense of generalized displacements and forces caused by specific type of external loading. The BEM is often used in the theory of both thin and thick plates and is particularly suitable for the analysis of the plates of arbitrary shapes resting on internal supports. The analysis of plate bending using BEM was introduced by Bèzine [3] and Stern [4] for Kirchhoff plate theory and by Vander Weeën [5] for the thick plate theory. Okupniak and Sygulski [6] used fundamental solution of Reissner plate proposed by Ganowicz [7]. Some authors present a modified approach to thin plate analysis. El-Zafrany, Debbih and Fadhil [8] assumed a non-zero distribution of stress over the plate thickness. Guminiak [9], [10], Guminiak, Okupniak and Sygulski [11] assumed a physical boundary condition also discussed in this paper. Modeling of the plate bending problem with internal plate supports requires a modification of the governing boundary integral equation. There are two methods known from literature, which usually take the internal supports into consideration. The most popular approach was proposed by Bèzine [12] in which, the forces at the internal supports are treated as unknown variables. This technique is also used by de Paiva and Venturini [13], [14], Hartmann and Zotemantel [15], Abdel-Akher and Hartley [16] and Gumniak and Sygulski [17]. Xiao [18] proposed BEM for the static analysis of Reissner plates resting on an internal elastic support of Winkler-type and elastic half-space. The second approach was proposed by Rashed [19] in the application of a coupled BEM-flexibility force method in the bending analysis of plates with internal supports.

## 2. BEM MODIFIED APPROACH

This paper includes a modified BEM formulation for the bending analysis of plates, in which three geometric and three static variables at the plate boundary are considered. In this approach there is no need to introduce the equivalent

shear forces at the boundary and concentrated forces at the plate corners. Internal elastic support was introduced using Bèzine techniques.

### 2.1. Integral formulation of thin plate bending

On the plate boundary three static variables are considered: the shear force  $T_n$ , the bending moment  $M_n$ , the torsion moment  $M_{ns}$  and three geometric variables: the deflection  $w$ , the angle of rotation in normal direction  $\varphi_n$  and the angle of rotation in the tangent direction  $\varphi_s$ . Only two of them are independent. The boundary integral equation is derived using the Bettie theorem. Two plates are considered: the infinite plate, subject to unit concentrated loading and the real one (Fig. 1).

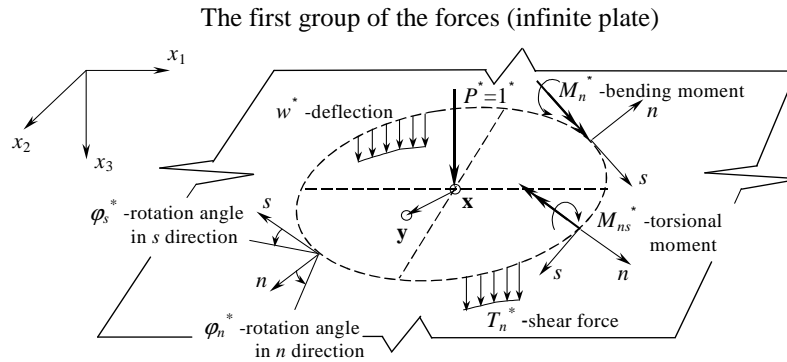
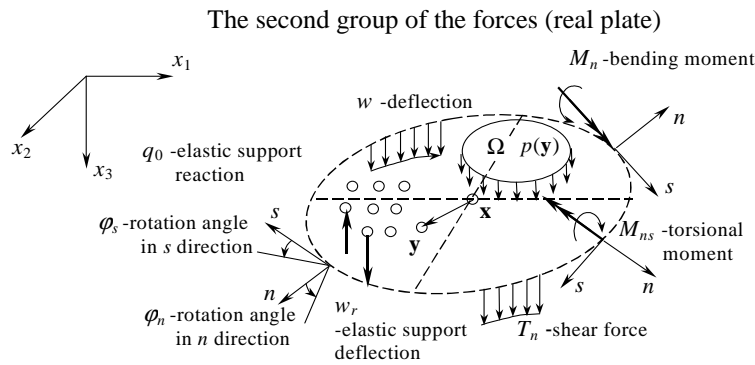


Fig. 1a. Variables present in the boundary integral equation: infinite plate



$\mathbf{x} = \mathbf{x}(x_1, x_2)$  – the source point

$\mathbf{y} = \mathbf{y}(x_1, x_2)$  – the field point

Fig. 1b. Variables present in the boundary integral equation: real plate

As a result, the boundary integral equation takes the form of

$$\begin{aligned}
& c(\mathbf{x}) \cdot w(\mathbf{x}) + \int_{\Gamma} \left[ T_n^*(\mathbf{y}, \mathbf{x}) \cdot w(\mathbf{y}) - M_n^*(\mathbf{y}, \mathbf{x}) \cdot \varphi_n(\mathbf{y}) - M_{ns}^*(\mathbf{y}, \mathbf{x}) \cdot \varphi_s(\mathbf{y}) \right] \cdot d\Gamma(\mathbf{y}) = \\
& = \int_{\Gamma} \left[ T_n(\mathbf{y}) \cdot w^*(\mathbf{y}, \mathbf{x}) - M_n(\mathbf{y}) \cdot \varphi_n^*(\mathbf{y}, \mathbf{x}) - M_{ns}(\mathbf{y}) \cdot \varphi_s^*(\mathbf{y}, \mathbf{x}) \right] \cdot d\Gamma(\mathbf{y}) + \\
& + \int_{\Omega} p(\mathbf{y}) \cdot w^*(\mathbf{y}, \mathbf{x}) \cdot d\Omega(\mathbf{y}) - \int_{\Omega_r} q_r(\mathbf{y}) \cdot w^*(\mathbf{y}, \mathbf{x}) \cdot d\Omega_r(\mathbf{y}),
\end{aligned} \tag{2.1}$$

where the fundamental solution of biharmonic equation

$$\nabla^4 w = \frac{1}{D} \cdot \delta(\mathbf{y} - \mathbf{x}), \tag{2.2}$$

is given as

$$w^*(\mathbf{y}, \mathbf{x}) = \frac{1}{D} \frac{r^2}{8\pi} \ln r, \tag{2.3}$$

for a thin isotropic plate,  $r = |\mathbf{y} - \mathbf{x}|$ ,  $\delta$  is Dirac delta and

$$D = \frac{E h^3}{12 (1 - \nu^2)}, \tag{2.4}$$

is the plate stiffness,  $h$  is the plate thickness,  $\nu$  is the Poisson's ratio,  $\Gamma$  denotes the plate boundary,  $\Omega$  denotes the loading area and  $\Omega_r$  denotes the elastic support area. The coefficient  $c(\mathbf{x})$  is assumed as

$$\begin{aligned}
c(\mathbf{x}) &= 1, & \text{when } \mathbf{x} \text{ is located inside the plate region,} \\
c(\mathbf{x}) &= 0.5, & \text{when } \mathbf{x} \text{ is located on the smooth boundary,} \\
c(\mathbf{x}) &= 0, & \text{when } \mathbf{x} \text{ is located outside the plate region.}
\end{aligned}$$

The second equation can be derived by substituting of the unit concentrated force  $\mathbf{P}^* = 1$  by the unit concentrated moment  $M_n^* = 1$ . It is equivalent to differentiate the first boundary integral equation (2.1) on  $n$  direction in point  $\mathbf{x}$  on the plate boundary.

$$\begin{aligned}
& c(\mathbf{x}) \cdot \varphi_n(\mathbf{x}) + \int_{\Gamma} \left[ \overline{T}_n^*(\mathbf{y}, \mathbf{x}) \cdot w(\mathbf{y}) - \overline{M}_n^*(\mathbf{y}, \mathbf{x}) \cdot \varphi_n(\mathbf{y}) - \overline{M}_{ns}^*(\mathbf{y}, \mathbf{x}) \cdot \varphi_s(\mathbf{y}) \right] \cdot d\Gamma(\mathbf{y}) = \\
& = \int_{\Gamma} \left[ T_n(\mathbf{y}, \mathbf{x}) \cdot \overline{w}(\mathbf{y}, \mathbf{x}) - M_n(\mathbf{y}) \cdot \overline{\varphi}_n(\mathbf{y}, \mathbf{x}) - M_{ns}(\mathbf{y}) \cdot \overline{\varphi}_s(\mathbf{y}, \mathbf{x}) \right] \cdot d\Gamma(\mathbf{y}) + \\
& + \int_{\Omega} p(\mathbf{y}) \cdot \overline{w}(\mathbf{y}, \mathbf{x}) \cdot d\Omega(\mathbf{y}) - \int_{\Omega_r} q_r(\mathbf{y}) \cdot \overline{w}(\mathbf{y}, \mathbf{x}) \cdot d\Omega_r(\mathbf{y}),
\end{aligned} \tag{2.5}$$

where

$$\begin{aligned} & \left\{ \overline{T_n^*}(\mathbf{y}, \mathbf{x}), \overline{M_n^*}(\mathbf{y}, \mathbf{x}), \overline{M_{ns}^*}(\mathbf{y}, \mathbf{x}), \overline{w^*}(\mathbf{y}, \mathbf{x}), \overline{\varphi_n^*}(\mathbf{y}, \mathbf{x}), \overline{\varphi_s^*}(\mathbf{y}, \mathbf{x}) \right\} = \\ & = \frac{\partial}{\partial n(\mathbf{x})} \left\{ T_n^*(\mathbf{y}, \mathbf{x}), M_n^*(\mathbf{y}, \mathbf{x}), M_{ns}^*(\mathbf{y}, \mathbf{x}), w^*(\mathbf{y}, \mathbf{x}), \varphi_n^*(\mathbf{y}, \mathbf{x}), \varphi_s^*(\mathbf{y}, \mathbf{x}) \right\}. \end{aligned} \quad (2.6)$$

In the equations (2.1) and (2.5) the additional part describing the behavior of the elastic support is included:  $\int_{\Omega_r} q_r(\mathbf{y}) \cdot w^*(\mathbf{y}, \mathbf{x}) \cdot d\Omega_r(\mathbf{y})$ .

## 2.2. Boundary conditions

In the calculations various kinds of plate edges were considered.

### 2.2.1. Clamped boundary

The boundary conditions are formulated as follows:

$$\begin{cases} w = 0 \\ \varphi_n = 0 \\ \varphi_s = 0 \\ M_{ns} = 0 \end{cases}. \quad (2.7)$$

The unknown variables are: the bending moment  $M_n$  and the shear force  $T_n$ .

### 2.2.2. Simply supported boundary

The boundary conditions are formulated as follows:

$$\begin{cases} w = 0 \\ \varphi_s = 0 \\ M_n = 0 \\ M_{ns} = 0 \end{cases}. \quad (2.8)$$

The unknown values are: the shear force  $T_n$  and the angle of rotation in direction  $n$ ,  $\varphi_n$ .

### 2.2.3. Free boundary

The boundary conditions are formulated as follows:

$$\begin{cases} T_n = 0 \\ M_n = 0 \\ M_{ns} = 0 \end{cases} \quad (2.9)$$

The unknown variables are: the deflection  $w$  and the angles of rotation  $\varphi_n$ ,  $\varphi_s$ . Because the relation between  $\varphi_s$  and  $w$  is known,  $\varphi_s = \frac{\partial w}{\partial s}$ , there are only two independent values:  $w$  and  $\varphi_n$ . After discretization of the plate boundary into constant elements having the same length, parameter  $\frac{\partial w}{\partial s}(\mathbf{y})$  can be calculated approximately by constructing a difference expression using the deflections of the three neighboring nodes (Fig. 2).

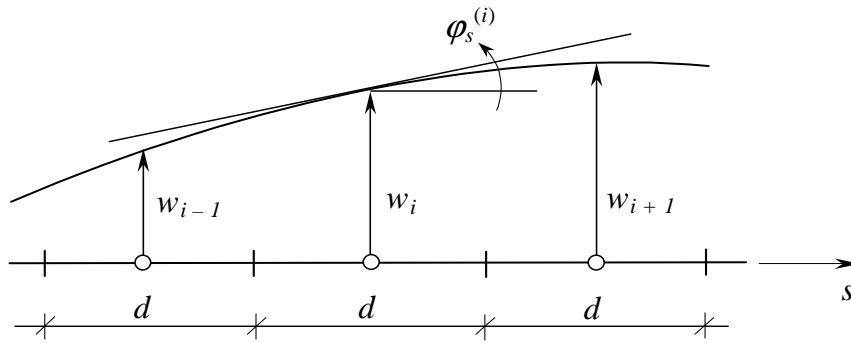


Fig. 2. Calculation of angle of rotation in the tangent direction

$$\varphi_s^{(i)} = \frac{1}{2d}(w_{i+1} - w_{i-1}), \quad (2.10)$$

$$\varphi_s^{(i-1)} = \frac{1}{d} \left( -\frac{3}{2}w_{i-1} + 2w_i - \frac{1}{2}w_{i+1} \right), \quad (2.11)$$

$$\varphi_s^{(i+1)} = \frac{1}{d} \left( \frac{1}{2}w_{i-1} - 2w_i + \frac{3}{2}w_{i+1} \right). \quad (2.12)$$

The expressions (3.5) and (3.6) are needed for the nodes located on the left and right end of the free boundary.

### 2.3. Discrete models of internal elastic support: Winkler-type and elastic half-space

Discrete models of elastic support have been considered: Winkler-type and elastic half-space. Deformation equation of elastic foundations (support) has the form (Fig. 3a.)

$$w_r(\mathbf{P}) = \int_{\Omega} q_r(\mathbf{Q}) \cdot g_r(\mathbf{P}, \mathbf{Q}) \cdot d\Omega_{r\mathbf{Q}}, \quad (2.13)$$

where  $q_r$  is the foundation reaction,  $\Omega_{r\mathbf{Q}}$  is the loaded area and  $g_r(\mathbf{P}, \mathbf{Q})$  is the flexibility functions of the foundations.

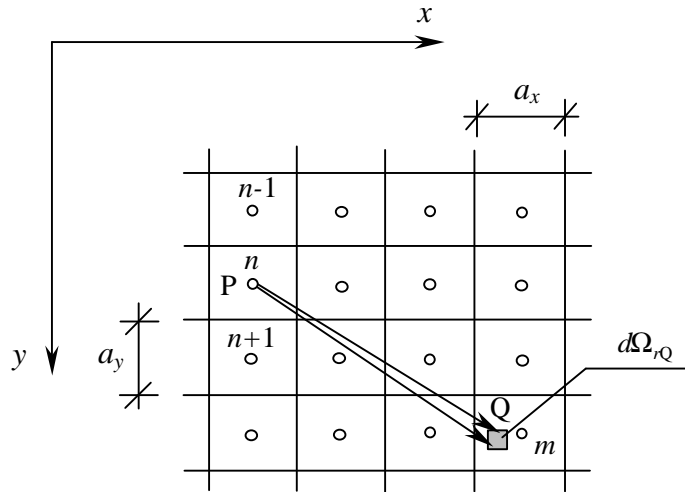


Fig. 3a. Construction of a foundation flexibility matrix

For Winkler-type foundation the flexibility function is

$$g_r(\mathbf{P}, \mathbf{Q}) = \frac{1}{k} \delta(\mathbf{P}, \mathbf{Q}), \quad (2.14)$$

where  $\delta(\mathbf{P}, \mathbf{Q})$  is Dirac delta and  $k$  is foundation stiffness.

For elastic half-space foundation, the flexibility function has the form of

$$g_r(\mathbf{P}, \mathbf{Q}) = \frac{1 - \nu_0^2}{\pi E_0} \cdot \frac{1}{r} = C_r \cdot \frac{1}{r}, \quad (2.15)$$

where  $E_0$  is the elastic modulus and  $\nu_0$  is the Poisson's ratio of the foundation.

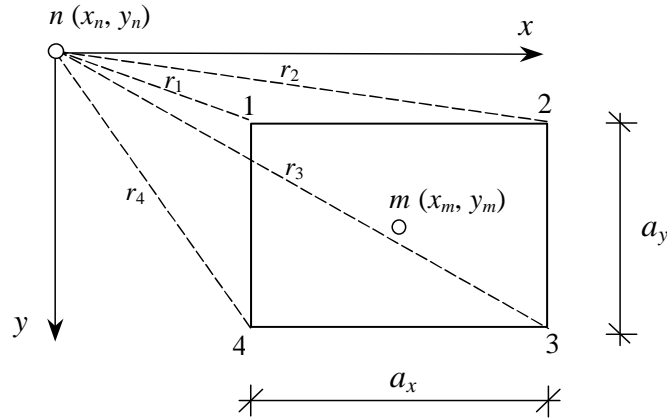


Fig. 3b. The calculation of the elements of matrix  $\mathbf{D}$  for elastic half-space

After discretization, the Winkler-type of the elastic foundation can be described by constructing a diagonal flexibility matrix with coefficients:  $(1/k) \cdot a_x a_y$ . For elastic half-space type of the foundation, the deformation function has the form (Fig. 3b.) of

$$w_n = C_r \cdot \sum_{m=1}^M q_{r,m} \cdot \int_{\Omega_m} \frac{1}{r_{n,Q}} \cdot d\Omega_Q \quad (2.17)$$

In the matrix notation

$$\mathbf{w} = C_r \cdot \mathbf{D} \cdot \mathbf{q}_r \quad (2.18)$$

where  $C_r \cdot \mathbf{D}$  is the flexibility matrix of the elastic foundation. For the type of elastic half-space, the matrix  $\mathbf{D}$  is fully-populated.

The elastic support reaction vector can be calculated using equation (4.5) and has the form

$$\mathbf{q}_r = \mathbf{K} \cdot \mathbf{w} \quad (2.19)$$

where  $\mathbf{K} = (1/C_r) \mathbf{D}^{-1}$ . Vector  $\mathbf{q}_r$  must be included in the boundary integral equations (2.1) and (2.5).

## 2.4. Construction of a set of algebraic equations

The plate is rested on the internal column supports and subjected by uniformly distributed loading  $p$  acting on the surface (Fig. 4a and 4b).

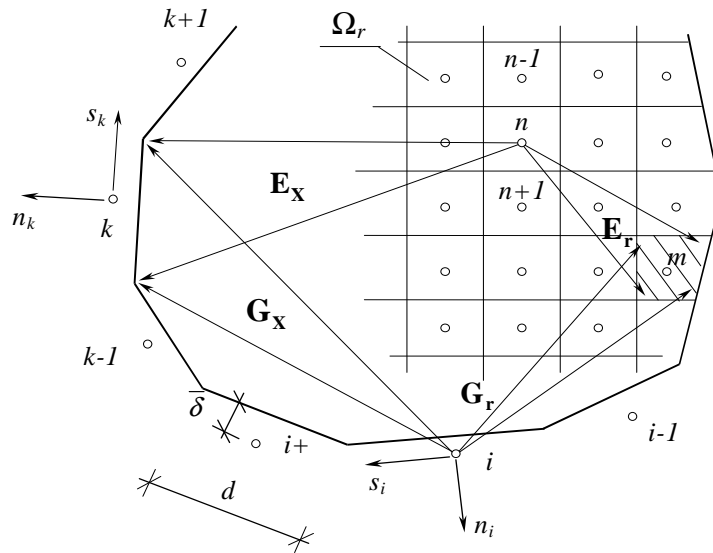


Fig. 4a. Construction of a set of algebraic equations: characteristic matrix

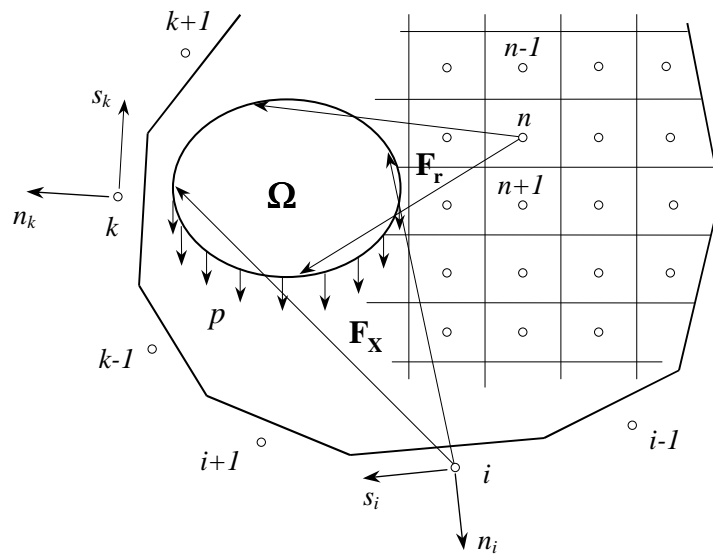


Fig. 4b. Construction of a set of algebraic equations: right-hand-side vector

The elements of characteristic matrix:  $\mathbf{G}_X$ ,  $\mathbf{E}_X$ ,  $\mathbf{G}_r$  and  $\mathbf{E}_r$  contain integrals of suitable fundamental functions depending on the type of the boundary.

These integrals are calculated in a local coordinate system  $n_i, s_i$  and then transformed to coordinate system  $n_k, s_k$ . The quasi-diagonal elements of the characteristic matrix were calculated analytically and the rest of them numerically using a 12-point Gauss quadrature. The elements of right-hand-side vectors  $\mathbf{F}_x$  and  $\mathbf{F}_r$  were calculated according to [20]. Vector  $\mathbf{X}$  contains boundary unknown variables dependent on suitable boundary conditions and vector  $\mathbf{w}_r$  contains displacements of the internal supports.

The set of algebraic equations can be written in the form

$$\begin{bmatrix} \mathbf{G}_x & \mathbf{G}_r \\ \mathbf{E}_x & \mathbf{E}_r \end{bmatrix} \begin{Bmatrix} \mathbf{X} \\ \mathbf{w}_r \end{Bmatrix} = \begin{Bmatrix} \mathbf{F}_x \\ \mathbf{F}_r \end{Bmatrix}. \quad (2.20)$$

## 2.5. Calculation of the displacement on a plate surface

The solution of the set of algebraic equations allowed to find suitable boundary variables, displacements and reactions in internal collocation points (internal elastic supports). Based on the same boundary integral equation (2.1) it is possible to calculate the displacement in an arbitrary point of a plate surface (the collocation point is located inside the plate region,  $c(\mathbf{x})=1$ ). The displacement in an arbitrary point of a plate region is given by the equation

$$w = w(\bar{\mathbf{X}}) + w(\mathbf{w}_r) + w(p), \quad (2.21)$$

or

$$w = w(\bar{\mathbf{X}}) + w(\mathbf{q}_r) + w(p). \quad (2.22)$$

Directly, from the boundary integral equation (2.1) it is possible to obtain

$$\begin{aligned} w(\mathbf{x}) = & - \int_{\Gamma} [T_n^*(\mathbf{y}, \mathbf{x}) \cdot w(\mathbf{y}) - M_n^*(\mathbf{y}, \mathbf{x}) \cdot \varphi_n(\mathbf{y}) - M_{ns}^*(\mathbf{y}, \mathbf{x}) \cdot \varphi_s(\mathbf{y})] \cdot d\Gamma(\mathbf{y}) + \\ & + \int_{\Gamma} [T_n(\mathbf{y}) \cdot w^*(\mathbf{y}, \mathbf{x}) - M_n(\mathbf{y}) \cdot \varphi_n^*(\mathbf{y}, \mathbf{x}) - M_{ns}(\mathbf{y}) \cdot \varphi_s^*(\mathbf{y}, \mathbf{x})] \cdot d\Gamma(\mathbf{y}) + \\ & + \int_{\Omega} p(\mathbf{y}) \cdot w^*(\mathbf{y}, \mathbf{x}) \cdot d\Omega(\mathbf{y}) - \int_{\Omega_0} q_0(\mathbf{y}) \cdot w^*(\mathbf{y}, \mathbf{x}) \cdot d\Omega_0(\mathbf{y}), \end{aligned} \quad (2.23)$$

and after discretization of the plate boundary into a finite number of constant type boundary elements

$$\begin{aligned}
w(x_1, x_2) = & -\sum_{k=1}^{le} w_k \cdot \int_{\Gamma_k} T_n^* \cdot d\Gamma_k + \sum_{k=1}^{le} \varphi_n \cdot \int_{\Gamma_k} M_n^* \cdot d\Gamma_k + \sum_{k=1}^{le} \varphi_s \cdot \int_{\Gamma_k} M_{ns}^* \cdot d\Gamma_k + \\
& + \sum_{k=1}^{le} T_n \cdot \int_{\Gamma_k} w^* \cdot d\Gamma_k - \sum_{k=1}^{le} M_n \cdot \int_{\Gamma} \varphi_n^* \cdot d\Gamma_k - \sum_m^M q_0(\mathbf{y}) \cdot \int_{\Omega_0} w^*(\mathbf{x}, \mathbf{y}) \cdot d\Omega_0 + \sum_{l=1}^{lp} p \cdot \int_{\Omega} w^* d\Omega, \quad (2.24)
\end{aligned}$$

where  $le$  is the number of boundary elements,  $M$  is the number of the internal collocation points (supports) and  $lp$  is the number of uniformly distributed loadings acting on the plate surface.

## 2.6. Calculation of the bending moments on a plate surface

Calculating of the bending moment in an arbitrary point of a plate is done approximately by constructing difference expression using a deflection of five points (Fig. 5.):

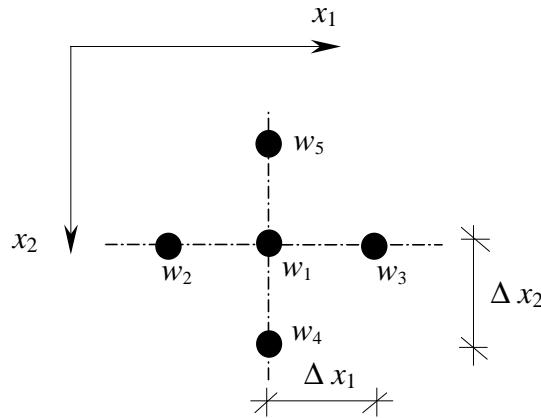


Fig. 5. Construction of difference expression

$$M_{x_1} = -D \left( \frac{\Delta^2 w}{\Delta x_1^2} + \nu_p \frac{\Delta^2 w}{\Delta x_2^2} \right), \quad (2.25)$$

and

$$M_{x_2} = -D \left( \frac{\Delta^2 w}{\Delta x_2^2} + \nu_p \frac{\Delta^2 w}{\Delta x_1^2} \right), \quad (2.26)$$

where

$$\frac{\Delta^2 w}{\Delta x_1^2} = \frac{w_2 - 2w_1 + w_3}{(\Delta x_1)^2}, \quad (2.27)$$

and

$$\frac{\Delta^2 w}{\Delta x_2^2} = \frac{w_4 - 2w_1 + w_5}{(\Delta x_2)^2}. \quad (2.28)$$

### 3. DIFFERENCE EQUATION FORMULATION IN THE FINITE STRIP METHOD

The concept of using of the finite strip methodology (FSM) for solving the static problem of an infinite plate strip resting on the internal elastic support has been presented. According to the FEM procedure, a plate strip of the width  $L$  is divided into a set of finite strips [21]. The regular mesh of identical finite strips of width  $b$  and length  $L$  approximates the continuous body (see Fig. 6).

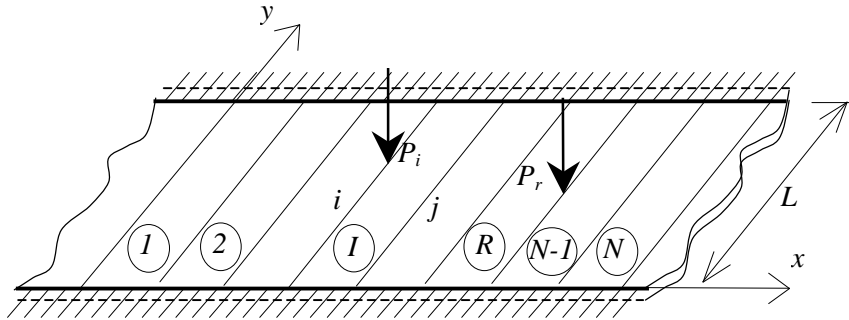


Fig. 6. The infinite plate strip discretization

The field of loading and displacement functions for an arbitrary strip  $I$ , is expressed in the combined form of harmonic series expansion

$$w^I(x, y) = \sum_{n=1}^{\infty} \mathbf{N} \cdot \mathbf{q}_n^I \sin \frac{n\pi y}{L}, \quad (3.1)$$

where:  $\mathbf{N} = [N_1 \quad N_2 \quad N_3 \quad N_4]^T$  is the shape functions vector:

$$N_1 = 1 - \frac{3x^2}{b^2} + \frac{2x^3}{b^3}, \quad N_2 = x - \frac{2x^2}{b} + \frac{x^3}{b^2}, \quad N_3 = \frac{3x^2}{b^2} - \frac{2x^3}{b^3}, \quad N_4 = -\frac{x^2}{b} + \frac{x^3}{b^2},$$

$\mathbf{q}_n^I = [w_{i,n} \ \phi_{i,n} \ w_{j,n} \ \phi_{j,n}]^T$  is the vector of displacement amplitudes for  $n$ -th harmonic (see Fig. 7).

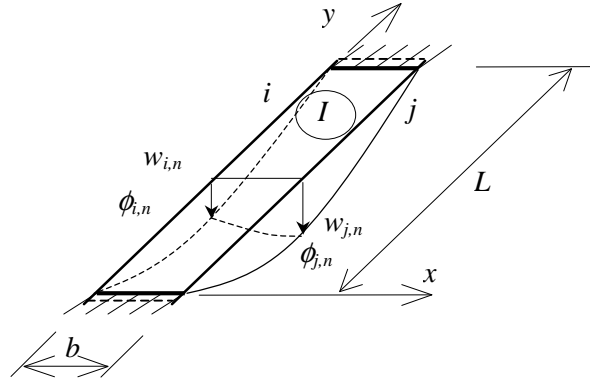


Fig. 7. The finite strip element

Displacements at the  $i$ -th nodal line are calculated in the form of the sum of amplitudes obtained for an arbitrary  $n$ -th element of the harmonic series

$$\begin{aligned} w_i &= \sum_{n=1}^{\infty} w_{i,n} \sin \frac{n\pi y}{L}, \\ \phi_i &= \sum_{n=1}^{\infty} \phi_{i,n} \sin \frac{n\pi y}{L}. \end{aligned} \quad (3.2)$$

### 3.1. Stiffness matrix

The finite strip stiffness matrix for the four-degree-of-freedom strip element takes the form [22] of

$$\mathbf{K}_n = (\alpha_1 + \alpha_k) \mathbf{K}_1 + \alpha_2 \mathbf{K}_2 + \alpha_3 \mathbf{K}_3 + \alpha_4 \mathbf{K}_4, \quad (3.3)$$

where

$$\begin{aligned} \alpha_1 &= \frac{\alpha_n^4 L b D_x}{840}, \quad \alpha_2 = \frac{L D_y}{b^3}, \quad \alpha_3 = \frac{\alpha_n^2 L D_1}{30b}, \quad \alpha_4 = \frac{\alpha_n^2 L D_{xy}}{30b}, \\ \alpha_k &= \frac{k}{420}, \quad \alpha_n = \frac{n\pi}{L}. \end{aligned}$$

The flexural stiffnesses for an orthotropic plate are:

$$D_x = \frac{E_x h^3}{12(1-\nu^2)}, \quad D_y = \frac{E_y h^3}{12(1-\nu^2)}, \quad D_1 = \frac{\nu(D_x + D_y)}{2}, \quad D_{xy} = \frac{D_x + D_y}{1-\nu}.$$

For the isotropic plate  $E_x = E_y = E$ , that means

$$D = D_x = D_y = \frac{Eh^3}{12(1-\nu^2)}, \quad D_1 = \nu D, \quad D_{xy} = \frac{2D}{(1-\nu)}, \quad E \text{ is the Young's modulus,}$$

$\nu$  is the Poisson's ratio,  $h$  is the plate thickness,  $k$  is the stiffness parameter of the Winkler-type foundation,  $\mathbf{K}_i$  are number matrices:

$$\mathbf{K}_1 = \begin{bmatrix} 156 & 22b & 54 & -13b \\ 22b & 4b^2 & 13b & -3b^2 \\ 54 & 13b & 156 & -22b \\ -13b & -3b^2 & -22b & 4b^2 \end{bmatrix}, \quad \mathbf{K}_2 = \begin{bmatrix} 6 & 3b & -6 & 3b \\ 3b & 2b^2 & -3b & b^2 \\ -6 & -3b & 6 & -3b \\ 3b & b^2 & -3b & 2b^2 \end{bmatrix},$$

$$\mathbf{K}_3 = \begin{bmatrix} 36 & 18b & -36 & 3b \\ 18b & 4b^2 & -3b & -b^2 \\ -36 & -3b & 36 & -18b \\ 3b & -b^2 & -18b & 4b^2 \end{bmatrix}, \quad \mathbf{K}_4 = \begin{bmatrix} 36 & 3b & -36 & 3b \\ 3b & 4b^2 & -3b & -b^2 \\ -36 & -3b & 36 & -3b \\ 3b & -b^2 & -3b & 4b^2 \end{bmatrix}.$$

### 3.2. The equilibrium conditions

The equilibrium equations are derived applying the finite element methodology. Assembling two adjacent elements  $R$  and  $R+1$  (see Fig. 8.) yields the equilibrium conditions at nodal line  $r$  for force's amplitudes of any harmonic  $n$  element

$$\begin{cases} T_{r,r-1} + T_{r,r+1} = P_r \\ m_{r,r-1} + m_{r,r+1} = m_r \end{cases}. \quad (3.4)$$

The equilibrium expression can be written for the regular system in the form of difference equations [23] equivalent to the FEM matrix formulation

$$\begin{cases} (\beta_1 \Delta^2 + \beta_0) w_r - \beta_2 (E - E^{-1}) \phi_r = \beta_p P_r \\ \beta_5 (E - E^{-1}) w_r + (\beta_3 \Delta^2 + \beta_4) \phi_r = \beta_m m_r \end{cases}. \quad (3.5)$$

where  $\Delta_r^2 = \Delta^2 = (E + E^{-1} - 2)$  is the second-order difference operator ( $\Delta^2 f_r = (E + E^{-1} - 2)f_r = f_{r+1} + f_{r-1} - 2f_r$ ),  $E_r^n = E^n$  is the shifting operator ( $E^n f_r = f_{r+n}$ ) [3],  $P_r$  and  $m_r$  are the forces and moments acting at the nodal line  $r$  (with  $y_p$  and  $y_m$  co-ordinates respectively)

$$\beta_p = \sin\left(\frac{n\pi y_p}{L}\right), \quad \beta_m = \sin\left(\frac{n\pi y_m}{L}\right),$$

$\beta_j$  are functions of geometrical and physical plate parameters.

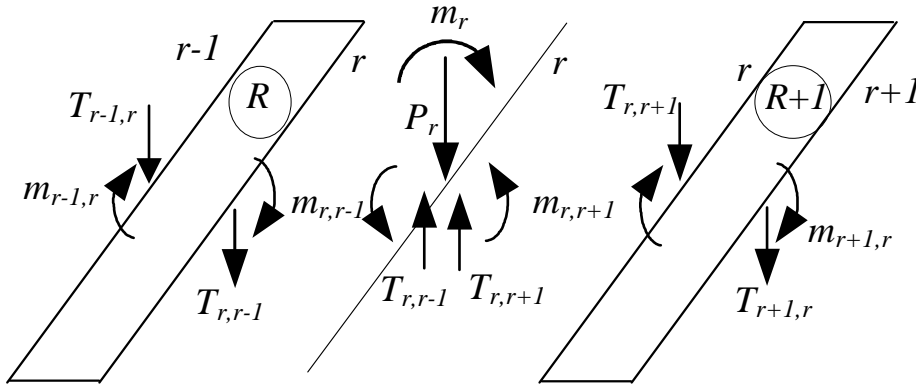


Fig. 8. The forces acting at nodal line  $r$

After the elimination of  $\phi_r$  in equation (3.5) it is possible to obtain a one fourth-order difference equation with one discrete unknown  $w_r$

$$\left[B_4\Delta^4 + B_2\Delta^2 + B_0\right] w_r = \beta_p \left[\beta_3\Delta^2 + \beta_4\right] P_r + \beta_2\beta_m (E - E^{-1}) m_r, \quad (3.6)$$

where

$$B_0 = \beta_0\beta_4, \quad B_2 = 4\beta_2\beta_5 + \beta_0\beta_3 + \beta_1\beta_4, \quad B_4 = \beta_2\beta_5 + \beta_1\beta_3,$$

$$\beta_0 = 420(\alpha_1 + \alpha_k), \quad \beta_1 = 6(9\alpha_1 - \alpha_2 - 6\alpha_3 - 6\alpha_4 + 9\alpha_k),$$

$$\beta_2 = b(13\alpha_1 - 3\alpha_2 - 3\alpha_3 - 3\alpha_4 + 13\alpha_k), \quad \beta_3 = b^2(-3\alpha_1 + \alpha_2 - \alpha_3 - \alpha_4 - 3\alpha_k),$$

$$\beta_4 = 2b(b\alpha_1 + 3b\alpha_2 + 3b\alpha_3 + b\alpha_k), \quad \beta_5 = b(13\alpha_1 - 3\alpha_2 - 3\alpha_3 - 3\alpha_4 + 13\alpha_k).$$

The set of an infinite number of equations formulated by FSM is replaced by one equation (3.6), which can be solved analytically.

### 3.3. The fundamental solution

The fundamental functions of  $w_r$  are found for the load  $P_0 = P_r \delta_{r,0}$ ,  $m_r = 0$  ( $\delta_{r,0}$  is Kronecker's delta) from a difference equation

$$[B_4 \Delta^4 + B_2 \Delta^2 + B_0] w_r = \beta_p [\beta_3 \Delta^2 + \beta_4] P_r. \quad (3.7)$$

For the regular mesh of the infinite plate strip we applied the discrete Fourier transform in  $x$ -direction

$$F^r [f_r] = \tilde{f}(\alpha) = \sum_{r=-\infty}^{\infty} f_r e^{ir\alpha}, \quad (3.8)$$

$$F^{-1} [\tilde{f}(\alpha)] = f_r = \frac{1}{2\pi} \int_{-\pi}^{\pi} \tilde{f}(\alpha) e^{-ir\alpha} d\alpha.$$

It gives the nodal displacement amplitude expression

$$w_r = \frac{P}{\pi} \int_0^{\pi} \frac{(S_1 \cos(\alpha) + S_2) \cos(r\alpha)}{\cos^2(\alpha) + B_m \cos(\alpha) + C_m} d\alpha, \quad (3.9)$$

where

$$B_m = (B_2 - 4B_4)/(2B_4), \quad C_m = (4B_4 - 2B_2 + B_0)/(4B_4),$$

$$S_1 = \beta_3 \beta_p / (2B_4), \quad S_2 = (\beta_4 - 2\beta_3) \beta_p / (4B_4).$$

Finally, the fundamental function (3.9) may be expressed in the form of the following recurrent relation

$$w_r = \frac{P}{\pi} [S_1 \cdot F_1(r) + S_2 \cdot F_2(r)], \quad (3.10)$$

where

$$F_1(r) = 2^{r-1} \cdot C(r+1) - \binom{r}{1} 2^{r-3} \cdot C(r-1) + \\ + \frac{r}{2} \binom{r-3}{1} 2^{r-5} \cdot C(r-3) - \frac{r}{3} \binom{r-4}{2} 2^{r-7} \cdot C(r-5) + \dots$$

$$F_2(r) = 2^{r-1} \cdot C(r) - \binom{r}{1} 2^{r-3} \cdot C(r-2) + \\ + \frac{r}{2} \binom{r-3}{1} 2^{r-5} \cdot C(r-4) - \frac{r}{3} \binom{r-4}{2} 2^{r-7} \cdot C(r-6) + \dots$$

The integrals

$$C(n) = \int_0^\pi \frac{\cos^n(\alpha)}{\cos^2(\alpha) + B_m \cos(\alpha) + C_m} d\alpha, \quad (3.11)$$

can be easily solved in an analytical way. The formula (3.10) expresses the deflection amplitude along the nodal line  $r$  for an arbitrary  $n$ -th element of harmonic series in a closed analytical form. From the equilibrium equations (3.5) we obtain the following relations for the transverse slope amplitudes

$$\theta_1 = -\frac{\beta_p P_r}{2\beta_2} + \frac{\beta_1}{\beta_2} w_1 - \frac{2\beta_1 - \beta_0}{2\beta_2} w_0, \quad (3.12) \\ \theta_{r+1} = \frac{2\beta_3 - \beta_4}{\beta_3} \theta_r - \theta_{r-1} - \frac{\beta_2}{\beta_3} (w_{r+1} - w_{r-1}).$$

The functions of displacements at the nodal line  $r$  are in the form of the sums

$$w(r, y) = \sum_{n=1}^N w_r(n) \cdot \sin \frac{n\pi y}{L}, \quad (3.13) \\ \theta(r, y) = \sum_{n=1}^N \theta_r(n) \cdot \sin \frac{n\pi y}{L},$$

where  $N$  is the number of harmonic elements,  $w_r(n)$  and  $\theta_r(n)$  are the amplitudes obtained from (3.10) and (3.12), respectively.

The fundamental functions (3.13) for the infinite strip allows to solve the static problem of the square plate according to the indirect BEM.

#### 4. NUMERICAL EXAMPLES

The square plates rested on the internal elastic support have been considered. Two types of elastic foundation have been considered: the Winkler-type and elastic half-space type. For the Winkler-type of foundation, unilateral type

of support (BEM approach) has also been considered, which is treated iteratively: points with negative reactions after the current step are eliminated in the following step. The BEM results are compared with the FSM ones and they are also verified using [18], [24], [25], [26]. To simplify, the designations accepted:  $x_1 = x$  and  $x_2 = y$ .

#### 4.1. A square plate with all simply-supported edges resting on the bilateral Winkler-type foundation subject to the uniformly distributed loading

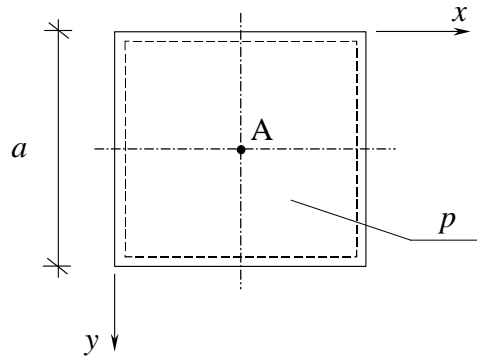


Fig. 6. A square plate resting on a Winkler-type of elastic support subject to the uniformly distributed loading  $p$

Plate and elastic support properties:

$a = 6.0$  m,  $h_p = 0.3$  cm,  $E_p = 30$  GPa,  $\nu_p = 0.16$ ,  $\varepsilon = \bar{\delta}/d = 0.001$ ,

$k = 50$  N/cm<sup>3</sup>, loading:  $p = 300$  kN/m<sup>2</sup>.

Number of boundary elements: 120,

number of internal collocation points: 100 (I), 400 (II).

Table 1. Deflection at the plate central point A

$w_{\max}$ [m]	
Type of foundation	Bilateral
<b>MEB – (I)</b>	$6.37156 \cdot 10^{-3}$
<b>MEB – (II)</b>	$6.36883 \cdot 10^{-3}$
<b>FSM</b>	$6.46114 \cdot 10^{-3}$

**4.2. A square plate with all simply-supported edges, resting on the bilateral Winkler-type foundation, subject to the patch load**

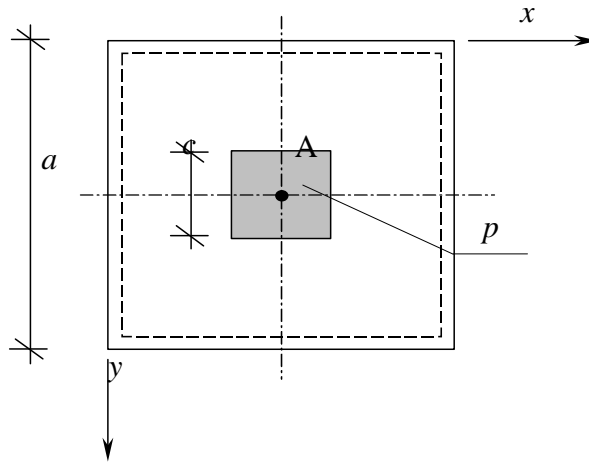


Fig. 7. A square plate resting on a Winkler-type of elastic support subject to the patch load  $p$

Plate and elastic support properties:

$a = 6.0$  m,  $c = 1.2$  m,  $h_p = 0.3$  cm,  $E_p = 30$  GPa,  $\nu_p = 0.16$ ,  $\varepsilon = \bar{\delta}/d = 0.001$ ,  
 $k = 50$  N/cm<sup>3</sup>, loading:  $p = 3000$  kN/m<sup>2</sup>.

Number of boundary elements: 120,

number of internal collocation points: 100 (I), 400 (II).

Table 2. Deflection at the plate central point A

$w_{\max}$ [m]	
Type of foundation	Bilateral
<b>MEB – (I)</b>	$8.50569 \cdot 10^{-3}$
<b>MEB – (II)</b>	$8.50258 \cdot 10^{-3}$
<b>FSM</b>	$8.49314 \cdot 10^{-3}$

**4.3. A square plate with two simply-supported opposite edges and two edges free, resting on the bilateral Winkler-type foundation, subject to the uniformly distributed loading**

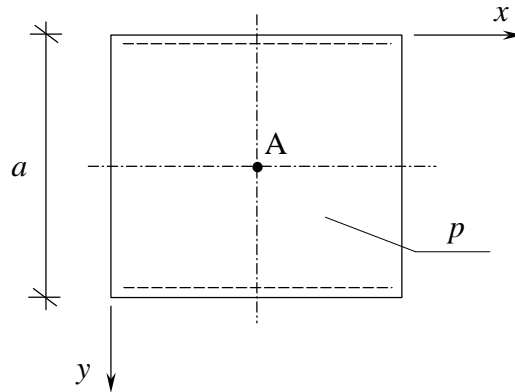


Fig. 8. A square plate resting on a Winkler-type of elastic support subject to the uniformly distributed loading  $p$

Plate and elastic support properties:

$a = 6.0$  m,  $h_p = 0.3$  cm,  $E_p = 30$  GPa,  $\nu_p = 0.16$ ,  $\varepsilon = \bar{\delta}/d = 0.001$ ,  
 $k = 50$  N/cm<sup>3</sup>, loading:  $p = 300$  kN/m<sup>2</sup>.

Number of boundary elements: 120,

number of internal collocation points: 100 (I), 400 (II).

Table 3. Deflection at the plate central point A

$w_{\max}$ [m]	
Type of foundation	Bilateral
<b>MEB – (I)</b>	$6.58294 \cdot 10^{-3}$
<b>MEB – (II)</b>	$6.59202 \cdot 10^{-3}$
<b>FSM</b>	$6.30416 \cdot 10^{-3}$

**4.4. A square plate with two simply-supported opposite edges and two edges free, resting on the bilateral Winkler-type foundation, subject to the patch load**

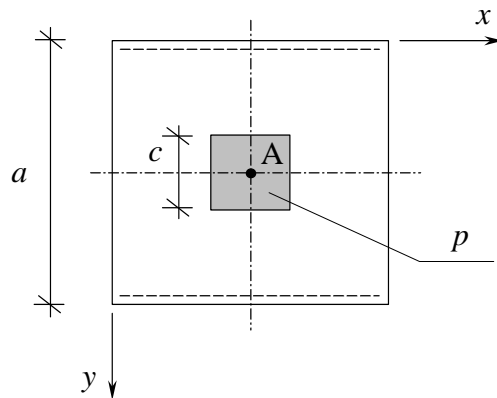


Fig. 9. A square plate resting on a Winkler-type of elastic support subject to the patch load  $p$

Plate and elastic support properties:

$a = 6.0$  m,  $c = 1.2$  m,  $h_p = 0.3$  cm,  $E_p = 30$  GPa,  $\nu_p = 0.16$ ,  $\varepsilon = \bar{\delta}/d = 0.001$ ,  
 $k = 50$  N/cm<sup>3</sup>, loading:  $p = 3000$  kN/m<sup>2</sup>.

Number of boundary elements: 120,

number of internal collocation points: 100 (I), 400 (II).

Table 4. Deflection at the plate central point A

$w_{\max}$ [m]	
Type of foundation	Bilateral
<b>MEB – (I)</b>	$8.52671 \cdot 10^{-3}$
<b>MEB – (II)</b>	$8.52522 \cdot 10^{-3}$
<b>FSM</b>	$8.50062 \cdot 10^{-3}$

**4.5. A square plate with two simply-supported opposite edges and two edges clamped, resting on the bilateral Winkler-type foundation, subject to the uniformly distributed loading**

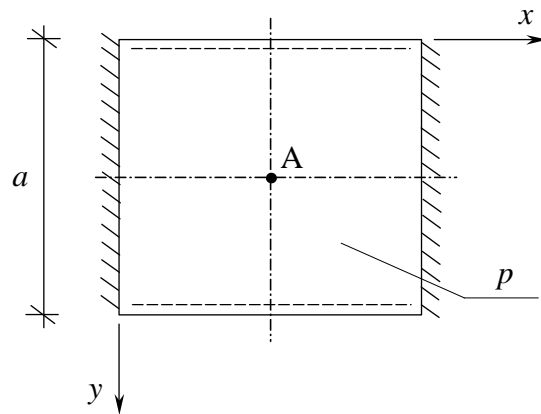


Fig. 10. A square plate resting on a Winkler-type of elastic support subject to the uniformly distributed loading  $p$

Plate and elastic support properties:

$a = 6.0$  m,  $h_p = 0.3$  cm,  $E_p = 30$  GPa,  $\nu_p = 0.16$ ,  $\varepsilon = \delta/d = 0.001$ ,

$k = 50$  N/cm<sup>3</sup>, loading  $p = 300$  kN/m<sup>2</sup>.

Number of boundary elements: 120,

number of internal collocation points: 100 (I), 400 (II).

Table 5. Deflection at the plate central point A

$w_{\max}$ [m]	
Type of foundation	Bilateral
<b>MEB – (I)</b>	$4.88544 \cdot 10^{-3}$
<b>MEB – (II)</b>	$4.88359 \cdot 10^{-3}$
<b>FSM</b>	$5.01424 \cdot 10^{-3}$

**4.6. A square plate with two simply-supported opposite edges and two edges clamped, resting on the bilateral Winkler-type foundation, subject to the patch load**

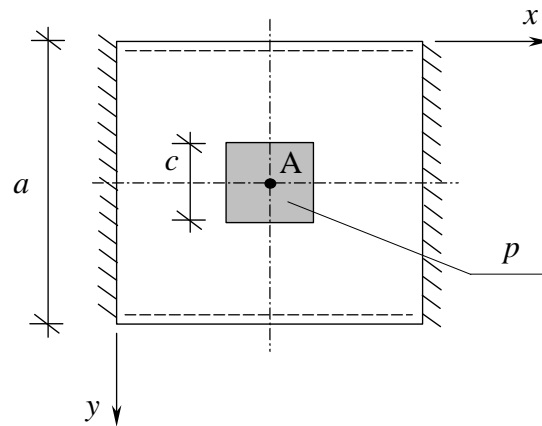


Fig. 11. A square plate resting on a Winkler-type of elastic support subject to the patch load  $p$

Plate and elastic support properties:

$a = 6.0$  m,  $c = 1.2$  m,  $h_p = 0.3$  cm,  $E_p = 30$  GPa,  $\nu_p = 0.16$ ,  $\varepsilon = \bar{\delta}/d = 0.001$ ,

$k = 50$  N/cm<sup>3</sup>, loading:  $p = 3000$  kN/m<sup>2</sup>.

Number of boundary elements: 120,

number of internal collocation points: 100 (I), 400 (II).

Table 6. Deflection at the plate central point A

$w_{\max}$ [m]	
Type of foundation	Bilateral
<b>MEB – (I)</b>	$7.59889 \cdot 10^{-3}$
<b>MEB – (II)</b>	$7.59643 \cdot 10^{-3}$
<b>FSM</b>	$7.60145 \cdot 10^{-3}$

#### 4.7. A square plate with all edges free resting on bilateral and unilateral Winkler-type of elastic foundation subject to the patch load

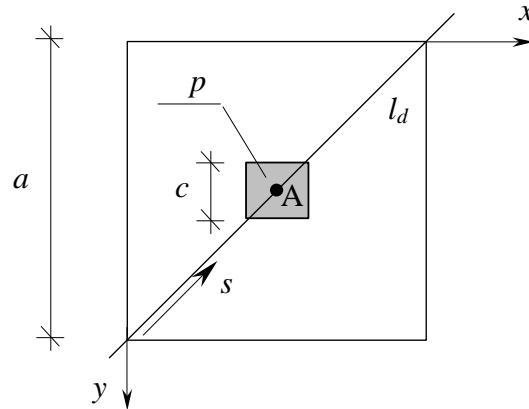


Fig. 12. A square plate resting on a Winkler-type of elastic support subject to the patch load  $p$

Plate and elastic support properties:

$a = 400$  cm,  $h_p = 20$  cm,  $E = 2.6 \times 10^6$  N/cm<sup>2</sup>,  $\nu_p = 0.15$ ,  $\varepsilon = \bar{\delta}/d = 0.001$ ,  
 $c = 50$  cm,  $k = 50$  N/cm<sup>3</sup>, loading:  $p = 300$  N/cm<sup>2</sup>.  
 Number of boundary elements: 64,  
 number of internal collocation points: 256.

Table 7. Deflection at the plate central point A

Type of foundation	$w_{\max}$ [cm]	
	Unilateral	Bilateral
<b>MEB</b> - present	0.333087	0.329574
Kirchhoff [24]	0.338520	0.333560
Kirchhoff [25]	0.333604	0.329870
Reissner [18]	0.346120	0.341456
Reissner [26]	0.341402	0.337788

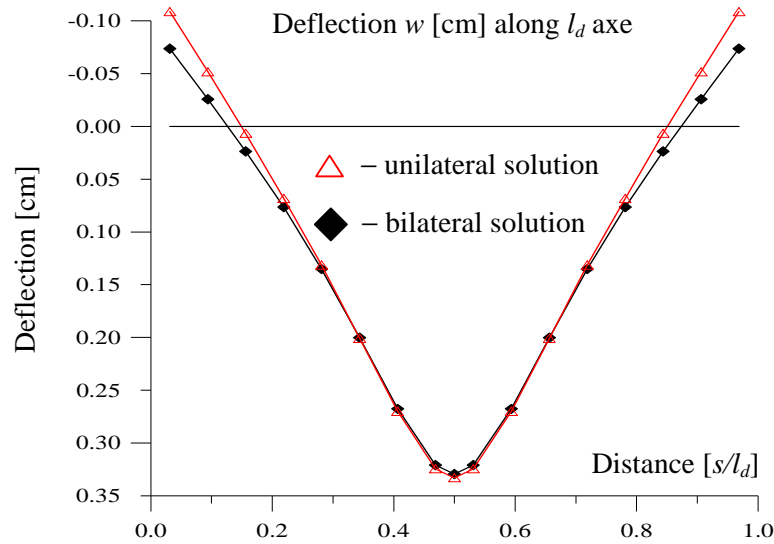


Fig. 13. A square plate resting on a Winkler-type of elastic support.  
Deflection along  $l_d$  axis

Table 8. Bending moment at the plate central point A

$M_{\max}$ [N·cm/cm] · 10 <sup>6</sup> , <b>MEB</b> - present	
Unilateral solution	Bilateral solution
0.116912	0.115320

Number of iteration – 3.

#### 4.8. A square plate with all edges free resting on elastic half-space-type of support, subject to the concentrated force at the center

Plate and elastic support properties:

$a = 100$  cm,  $h_p = 2$  cm,  $E = 2.6 \times 10^6$  N/cm<sup>2</sup>,  $\nu_p = 0.3$ ,  $\varepsilon = \delta/d = 0.001$ ,

$E_0 = 3000$  N/cm<sup>2</sup>,  $\nu_0 = 0.3$ , loading:  $P = 1000$  N.

Number of boundary elements: 64,

number of internal collocation points (internal sub-surfaces): 256.

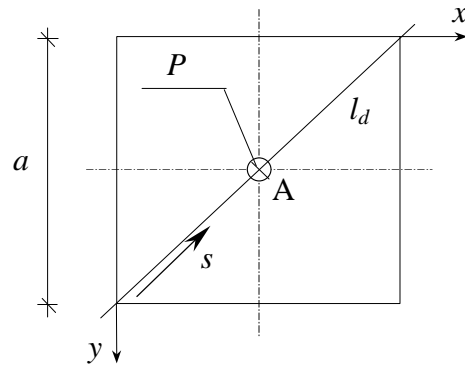


Fig. 14. A square plate resting on a elastic half-space subject to the concentrated force P

Table 9. Deflection at the plate central point A

$w_{\max}$ [cm]	
<b>BEM - present</b>	[18]
0.01209	0.0107

Table 10. Internal support reaction near the center point A

$q_{r \max}$ [N/cm <sup>2</sup> ]	
<b>BEM - present</b>	[18]
1.50972	1.60

Table 11. Bending moment at the plate center point A

$M_{\max}$ [N·cm/cm] · 10 <sup>3</sup>
<b>MEB - present</b>
0.281743

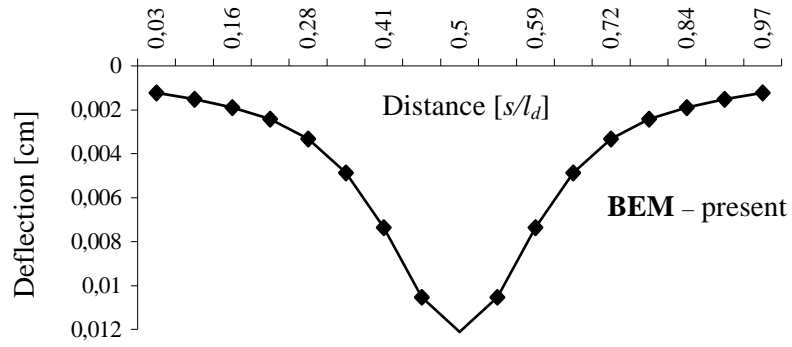


Fig. 15. BEM results – present. Deflection along  $l_d$  axis

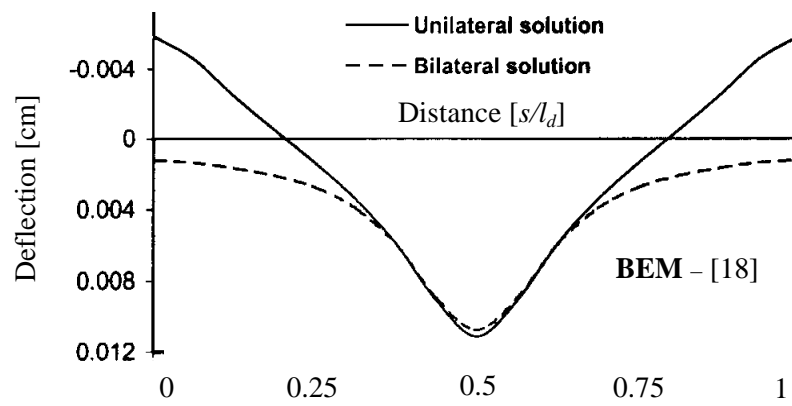


Fig. 16. BEM results – [18]. Deflection along  $l_d$  axis

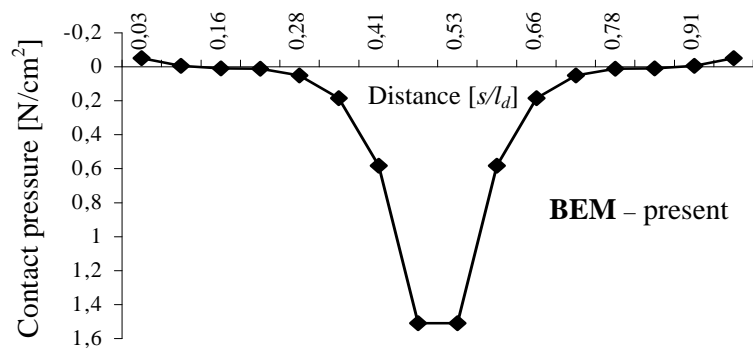


Fig. 17. BEM results – present. Contact pressure along  $l_d$  axis

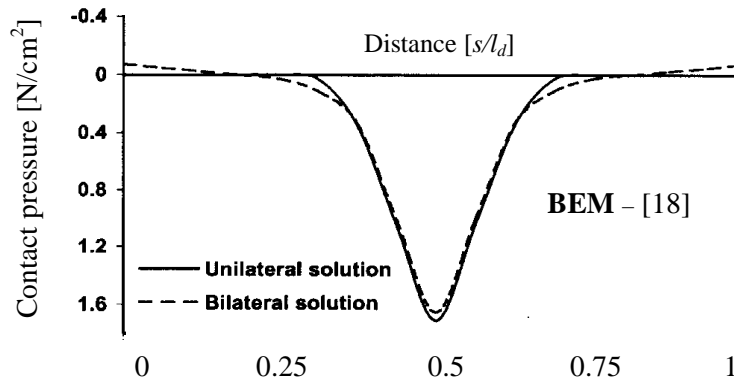


Fig. 18. BEM results – [18]. Contact pressure along  $l_d$  axe

## 5. CONCLUSIONS

A static analysis of thin plates resting on internal elastic supports using the Boundary Element Method and Finite Strip Method has been presented. In the BEM modified approach, there is no need to introduce the Kirchhoff forces at the plate corners and the equivalent shear forces at the plate boundary. The collocation version of BEM with constant type elements and non-singular calculations of integrals have been employed. The source points of the boundary elements are located slightly outside the plate boundary, hence all of the integrals of the fundamental function are non-singular. The displayed BEM results demonstrate the effectiveness and efficiency of the proposed approach. This method can also be applied to a static analysis of plates resting on an internal column support and a free vibration analysis of thin plates. The obtained BEM numerical results were compared with the FSM and other BEM numerical ones.

## BIBLIOGRAPHY

1. Brebbia, C.A., Telles, J.C.F. and Wrobel, L.C.: Boundary Element Techniques, Theory and Applications in Engineering, Springer-Verlag, Berlin Heidelberg, New York, Tokyo, 1984.
2. Burczyński T.: The Boundary Element Method in Mechanics, Technical-Scientific Publishing house, Warszawa, 1995 (in Polish).

3. Bèzine G.: Boundary integral formulation for plate flexure with arbitrary boundary condition, *Mechanics Research Communications*, **5**(4) (1978), 197-206.
4. Stern M.: A general boundary integral formulation for the numerical solution of plate bending problems, *Int. J. Solids Structures* **15** (1979), 169-782.
5. Vander Weeën F.: Application of the boundary integral equation method to Reissner's plate model, *Int. J. Num. Meth. Engng.*, **18** (1982) 1-10.
6. Okupniak B, Sygulski R.: Non-singular BEM analysis of Reissner plates, *Proceedings of 15<sup>th</sup> International Conference on Computer Methods in Mechanics CMM-2003*, 3-6 June 2003, Gliwice/Beskidy Mountains, Poland, 265-266.
7. Ganowicz R.: Some questions of theory Reissner and three-layers plates, *Theoretical and Applied Mechanics*, 1966 (in Polish).
8. El-Zafrany A., Debbih M. and Fadhil S.: A modified Kirchhoff theory for boundary element bending analysis of thin plates, *Int. J. Solids Structures*, **21** (31) (1994), 2885- 2889.
9. Guminiak M.: Application of the boundary element method in static analysis of thin plates (in Polish), 3<sup>rd</sup> Scientific Conference of PhD Students of Civil Engineering, Gliwice-Wisła, 21-22 November, 2002, Silesian University of Technology, Poland, 223-232.
10. Guminiak M.: Thin plates analysis by the boundary element method using new formulation of a boundary condition (in Polish), PhD Thesis, Poznan University of Technology, Poznan, Poland, 2004.
11. Guminiak M., Okupniak B., Sygulski R.: Analysis of plate bending by boundary element method, 2<sup>nd</sup> European Conference on Computational Mechanics ECCM-2001, June 26-29, Cracow, Poland, 1, 2001, 176-177.
12. Bezine G.: A boundary integral equation method for plate flexure with condition inside the domain, *Int. J. Num. Meth. Engng.* **15** (1981), 1647-1657.
13. de Paiva J. B., Venturini W. S.: Boundary element algorithm for building floor slab analysis, In *International Conference of BETECH 85*, Adelaide, Australia, Brebbia C. A., Noye B. J. (eds), *Computational Mechanics Publications* (1985), 201-209.
14. de Paiva J. B., Venturini W. S.: Analysis of building structures considering plate-beam-column interactions, In *International Conference of BETECH 87*, Rio de Janeiro, Brazil, Brebbia C. A., Venturini W. S. (eds), *Computational Mechanics Publications* (1987), 209-219.
15. Hartmann F., Zotemantel R.: The direct boundary element method in plate bending, *Int. J. Num. Meth. Engng.*, **23** (1986), 2049-2069.
16. Abdel-Akher A., Hartley G. A.: Evaluation of boundary integrals for plate bending. *Int. J. Num. Meth. Engng.*, **28** (1989), 75-93.

17. Guminiak M., Sygulski R.: The analysis of internally supported thin plates by the Boundary Element Method. Part1-Static analysis, *Foundation of Civil and Environmental Engineering*, 9, (2007), 17-41, Poznan University of Technology, Poznan, Poland.
18. Xiao J. R.: Boundary element analysis of unilateral supported Reissner plates on elastic foundations, *Computational Mechanics*, 27 (2001), 1-10.
19. Rashed Y. F.: A coupled BEM-flexibility force method for bending analysis of internally supported plates. *Int. J. Num. Meth. Engng.*, 54 (2002), 1431-1457.
20. Abdel-Akher A., Hartley G. A.: Domain integration for plate bending analysis by the boundary element method, *Applied Numerical Method*, 5 (1989), 23-28.
21. Loo Y. C., Cusens A. R., *The Finite Strip Method in Bridge Engineering*, New York, Viewpoint Publications, 1978.
22. Z. Pawlak, J. Rakowski : *Dynamic analysis of infinite plate strip by the finite strip method*. 16<sup>th</sup> International Conference on Computer Methods in Mechanics CMM-2005, Częstochowa, Poland, 21-24 June 2005, pp. 183-184.
23. Rakowski J., *The interpretation of the shear locking in beam elements*. *Comp. Structures*, 37, (1990), 769-776.
24. Li H., Dempsey J. P.: Unbonded contact of a square plate on a elastic half-space or a Winkler foundation, *ASME, J. Appl. Mech.*, 55 (1988), 430-436.
25. Bathe K. J., Chaudary A. B.: A solution method for planar and axisymmetric contact problems, *International Journal of Numerical Method in Engineering*, 21 (1985), 65-88.
26. Bu X.M., Yan Z.D., Bending problems of rectangular thin plate with free edges laid on tensionless Winkler foundation, *Appl. Math. Mech.*, 10(5) (1989), 435-442.